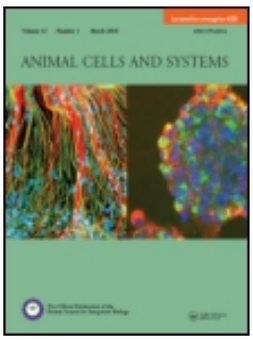

Taylor & Francis
Taylor & Francis Group

Animal Cells and Systems

ISSN: 1976-8354 (Print) 2151-2485 (Online) Journal homepage: https://www.tandfonline.com/loi/tacs20

Differential expression of four $Ca_V3.1$ splice variants in the repeat iii-iv loop

Sang-Soo Lee , You-Mi Park , Ho-Won Kang , Hyoweon Bang , Seong-Woo Jeong & Jung-Ha Lee

To cite this article: Sang-Soo Lee , You-Mi Park , Ho-Won Kang , Hyoweon Bang , Seong-Woo Jeong & Jung-Ha Lee (2008) Differential expression of four $Ca_V3.1$ splice variants in the repeat iii-iv loop, Animal Cells and Systems, 12:3, 137-141, DOI: 10.1080/19768354.2008.9647166

To link to this article: https://doi.org/10.1080/19768354.2008.9647166

Animal Cells and Systems 12: 137-141, 2008

Animal Cells and Systems
http://www.AnimalCells.or.kr

Differential Expression of Four $Ca_v3.1$ Splice Variants in the Repeat III-IV Loop

Sang-Soo Lee[1], You-Mi Park[1], Ho-Won Kang[1], Hyoweon Bang[3], Seong-Woo Jeong[4], and Jung-Ha Lee[1,2,*]

[1]*Department of Life Science,* [2]*Interdisciplinary Program of Integrated Biotechnology, Sogang University, Seoul 121-742, Korea;* [3]*Department of Physiology, Chung-Ang University, Seoul 156-756, Korea;* [4]*Department of Physiology, Yonsei University Wonju College of Medicine, Wonju 220-710, Korea*

Abstract: Molecular cloning revealed the three isoforms ($Ca_v3.1$, $Ca_v3.2$, and $Ca_v3.3$) of the T-type calcium channel subfamily. Expression studies exhibited their distinctive electrophysiological and pharmacological properties, accounting for diverse properties of T-type calcium channel currents previously characterized from isolated cells. However, electrophysiological properties of ion channels have shown to be more diversified by their splice variants. We here searched splice variants of rat $Ca_v3.1$ T-type channel by reverse-transcription-polymerase chain reaction (RT-PCR) to further explore diversity of $Ca_v3.1$. Interestingly, analyses of cloned RT-PCR products displayed that there were at least four splicing variants of rat $Ca_v3.1$ in the loop connecting repeats III and IV. Southern blot analyses indicated that the predominantly detected variant in brain was $Ca_v3.1a$ (492 bp), which were rarely detected in most of peripheral tissues. Other two variants ($Ca_v3.1c$, 546 bp; $Ca_v3.1d$, 525 bp) were detected in most of the tissues examined. The smallest isoform ($Ca_v3.1b$, 471 bp) was rarely detected all the tissues. Electrophysiological characterization of the splicing variants indicated that the splice variants differ in inactivation kinetics and the voltage dependence of activation and inactivation as well.

Key words: $Ca_v3.1$ T-type channel, alternative splicing, III-IV loop, Southern blot, voltage clamping

Low voltage-activated T-type Ca^{2+} channels have been thought to play crucial physiological roles such as pacemaking activities, rebound bursting, hormone secretion, acrosome reaction, muscle contraction, and cell differentiation (Huguenard, 1996; Lory et al., 2006; Park et al., 2003; Perez-Reyes, 2003; Suzuki and Rogawski, 1989). Molecular cloning and expression studies demonstrated existence of a T-type Ca^{2+} channel subfamily consisting of the three isoforms: $Ca_v3.1$, $Ca_v3.2$, and $Ca_v3.3$ (Cribbs et al., 1998; Lee et al., 1999a; Perez-Reyes et al., 1998; Perez-Reyes, 2003).

The specific physiological roles of $Ca_v3.1$ were identified by characterizing $Ca_v3.1$-knock-out mice which were shown to be deficient in burst firing of thalamocortical relay neurons and resistant to the generation of absence seizures in response to baclofen (Kim et al., 2001). In addition, $Ca_v3.1$-knock-out mice were reported to exhibit hyperalgesia in response to visceral pain, suggesting that $Ca_v3.1$ is involved in an antinociceptive mechanism operating in the thalamus (Kim et al., 2003). Differently, $Ca_v3.2$-knock-out mice were characterized to show abnormal relaxation of coronary arteries (Chen et al., 2003), and single nucleotide polymorphisms of $Ca_v3.2$ were linked with childhood absence epilepsy and generalized epilepsy syndromes (Heron et al., 2007; Vitko et al., 2005).

The common electrophysiological properties which cloned T-type Ca^{2+} channels share with native T-type currents are activation at negative potentials around –60 mV, slow deactivation kinetics, tiny single channel conductance at 100 mM barium, and the distinctive criss-crossing pattern of current traces during current-voltage protocols. Meanwhile, cloned three T-type channels can be differently characterized by following properties: (i) the activation and inactivation kinetics of $Ca_v3.1$ and $Ca_v3.2$ are several fold faster than those of $Ca_v3.3$; (ii) $Ca_v3.2$ is the only isoform selectively inhibited by metallic divalent ions such as nickel, zinc, and copper among the three T-type channel isoforms (Jeong et al, 2003; Lee et al, 1999b; Nelson et al., 2007).

Electrophysiological and pharmacological properties of numerous voltage-gated ion channels such as high voltage-activated calcium channels, potassium channels, ligand

* To whom correspondence should be addressed.
Tel: +82-2-705-8791; Fax: +82-2-704-3601
E-mail: jhleem@sogang.ac.kr

gated channels have shown to be extensively differentiated by α_1 subunit splice variants, auxiliary subunits, and their combination (Bourinet et al., 1999; Chen et al., 2005; Gros et al., 2002; Koshimizu and Tsujimoto, 2006; Takahashi et al., 2003; Welling et al., 1997). Although molecular cloning of three members of low-voltage activated T-type channels explained heterogeneity of T-type channel currents recorded from isolated cells, the electrophysiological properties of T-type channel currents could be much more broadened depending on those factors including splice variants, unidentified auxiliary subunits, and their combination.

In the present study, we designed PCR primers to amplify cytoplamic loops connecting repeats III and IV. Analysis of PCR products showed that there were four splicing variants of rat $Ca_v3.1$ in the III-IV loop. Southern blot and voltage clamping analyses strongly suggested that the splicing variants were differential distributed between the tissues with different biophysical properties.

MATERIALS AND METHODS

Isolation of total RNA and Reverse Transcription-Polymerase Chain Reaction (RT-PCR)

Total RNA was individually isolated from rat brain, heart, lung, kidney, skeletal muscle, and testis using the guanidium thiocyanate-phenol extraction (Chomczynski and Sacchi, 1987). First strand cDNA was reverse-transcribed from 0.5 μg of total RNA isolated from rat brain, heart, kidney, lung, skeletal muscle, or testis using MMuLV reverse transcriptase (Fermentas, Hanover, MD, USA). PCR was performed based on the cDNA using the following cycles: 1 cycle at 95°C for 1 min, 33 cycles composed of 30 sec at 94°C, 30 sec at 58°C, and 30 sec at 72°C. The PCR primers used in the reaction were based on the S6 segment of repeat III and the pre-S4 region of repeat IV and their sequences were as follows: the forward primer, GCGTGGTGGTGGAGAACTT, and the reverse primer, GATGATGGTGGG(A/G)TTGAT. PCR products were cloned into pCR2.1 TOPO (Invitrogen, Carlsbad, CA, USA) and then cloned sequences were verified by automatic sequencing.

Southern blot analyses

PCR products were separated through a 2% Nuseive 3:1 agarose gel containing 1 μg/ml of ethidium bromide by electrophoresis. Separated products were transferred to a nylon membrane (Hybond-N, Amersham, Piscataway, NJ, USA). The membrane was hybridized at 40°C with rat $Ca_v3.1$-specific oligonucleotides (AGATTCCGGCTCCTT GTCCACCAC), which were labeled with ^{32}P-ATP by T4 polynucleotide kinase (Fermentas, Hanover, MD, USA). The final wash was in a 0.5×SSC and 0.1% SDS at 55°C. The membrane was exposed to an X-ray film for 1 min.

Construction of the full-length cDNAs of $Ca_v3.1$ splicing variants in the III-IV loop

Construction of the full-length cDNA of rat $Ca_v3.1a$ in pGEM-HEA was previously reported (GenBank accession number AF027984; Lee et al., 1999a). RT-PCR was performed from rat kidney RNA to obtain $Ca_v3.1b$, $Ca_v3.1c$, and $Ca_v3.1d$ cDNA sequences containing *Eco*RI (4199) to *Bgl*II (4817). The forward primer was ATTGGC AACATTGTGGTCATTTG and the reverse primer was GATGATGGTGGG(A/G)TTGAT. To construct the full-length clones of the variants, a rat $Ca_v3.1$ fragment (*Eag*I (3598)/*Eco*RI (4199)) and the PCR products digested with *Eco*RI and *Bgl*II (4817), were subcloned into $Ca_v3.1a$-pGEMHEA digested with *Eag*I (3598) and *Bgl*II (4817). The full-length construct were checked by restriction enzyme digestion and sequencing.

Expression and electrophysiological characterization of the $Ca_v3.1$ III-IV loop variants

The $Ca_v3.1$ variants were reconstituted in oocytes prepared from mature female *Xenopus laevis* (*Xenopus* Express, France) (Lee et al., 1999a). The splice variant cDNAs were individually linerized by *Afl*II and their complementary RNAs were synthesized using T7 RNA polymerase according to the protocol supplied by the manufacturer (Ambion, Austin, TX, USA) and then injected into *Xenopus* oocytes. Barium currents through expressed channels were measured the third day after cRNA injection using a two-electrode voltage-clamp amplifier (OC-725C, Warner Instruments, Hamden, CT, USA). The 10 mM Ba^{2+} bath solution contained (mM): 10 $Ba(OH)_2$, 90 NaOH, 1 KOH, 5 Hepes (pH 7.4 with methanesulphonic acid). The currents were usually sampled at 5 kHz and low pass filtered at 1 kHz using the pCLAMP system (Digidata 1320A and pCLAMP 8; Axon Instruments, Union City, CA, USA). Peak currents and exponential fits to currents were analyzed using Clampfit software (Axon Instruments, Sunnyvale, CA, USA) and presented graphically using Prism software (GraphPad, San Diego, CA, USA). Data are presented as means±S.E.M. and tested for significance using one-way ANOVA test with $P<0.05$ and $P<0.01$ as levels of significance.

RESULTS AND DISCUSSION

In an effort to clone splicing variants of rat $Ca_v3.1$ T-type channels, we have performed RT-PCR for which primers were designed on the basis on conserved sequence in all three mammalian T-type calcium channels. One pair of primers corresponding to the S6 segment of repeat III and the pre-S4 region of repeat IV amplified PCR products which appeared to slightly differ in size on an agarose gel, suggesting existence of multiple splice variants of rat

Fig. 1. Alternative splicing variants of the rat $Ca_v3.1$ in the III-IV linker. A, Sequence alignment of the $Ca_v3.1$ splice variants. Rat $Ca_v3.1$ clones amplified by RT-PCR were sequenced and deduced into amino acid sequences. The III-IV loop sequences of the four $Ca_v3.1$ splice variants were aligned with previously cloned Ca^{2+} channels, but the sequences corresponding to the repeat IV S1-S3 were omitted in the alignment. $Ca_v3.1a$ is identical to the rat $Ca_v3.1$ which was first cloned (Perez-Reyes et al., 1998; Genbank access no AF027984). $Ca_v3.1b$ is a shorter variant, while $Ca_v3.1c$ and $Ca_v3.1d$ are longer variants than $Ca_v3.1a$. The Genbank accession numbers of the other Ca^{2+} channel sequences were: human $Ca_v3.2$, NM 021098; rat $Ca_v3.3$, AF086827; human $Ca_v1.1$, NM 000069; human $Ca_v1.2$, NM 199460; human $Ca_v2.1$, X99897; and human $Ca_v2.3$, L27745. B, Alternative splicing models of the four $Ca_v3.1$ variants. The four splice variants ($Ca_v3.1a$, $Ca_v3.1b$, $Ca_v3.1c$, and $Ca_v3.1d$) in the III-IV linker are generated from the same gene by alternative splicing(s), of which models were schematically represented. The boxes represent exons and the gaps between boxes do introns.

$Ca_v3.1$. The PCR products were cloned and then sequenced for identification. Analyses of the DNA sequences represented that there exist at least four splice variants of rat $Ca_v3.1$, being named $Ca_v3.1a$, $Ca_v3.1b$, $Ca_v3.1c$, and $Ca_v3.1d$. $Ca_v3.1a$ was 492 base pairs (bp), identical to the first cloned $Ca_v3.1$ (Perez-Reyes et al., 1998; GenBank accession number AF027984), while $Ca_v3.1b$, $Ca_v3.1c$, and $Ca_v3.1d$ were 471, 546, and 525 bp, respectively.

The DNA sequences of the four variants were deduced into amino acid sequences, and then aligned with the corresponding sequences of other voltage-gated calcium channels in the III-IV linker region (Fig. 1A). Comparison of deduced sequences exhibited that compared to $Ca_v3.1a$, $Ca_v3.1b$ missed "SKEKQMA" (Ser-Lys-Glu-Lys-Gln-Met-Ala) in the III-IV linker. In contrast, $Ca_v3.1c$ and $Ca_v3.1d$ contained 18 and 11 amino acids more than $Ca_v3.1a$, respectively. Comparison of the genomic sequence of rat and human $Ca_v3.1$ and their cDNA sequences in the III-IV linker region suggested how the four splice variants are generated by alternative splicing(s), which were schematically diagramed (Fig. 1B).

One of the questions raised is whether the four splice variants are differently expressed among tissues. To examine the question, we employed Southern blot analyses for which RT-PCR products from rat tissue RNAs were separated on a gel, transferred to a nylon membrane, and then screened with probes specific to the rat $Ca_v3.1$. The predominantly detected variant in rat brain was $Ca_v3.1a$ (492 bp), which was little detected on the other tissues including heart, kidney, lung, skeletal muscle, and testis. $Ca_v3.1c$ and $Ca_v3.1d$ variants (546 and 525 bp) were detected in all the tissues examined, except weak detection of $Ca_v3.1d$ in heart. The smallest form ($Ca_v3.1b$, 471 bp) was rarely detected over the tissues examined (Fig. 2). These findings suggest that the four variants are differentially expressed between the tissues, possibly via different alternative splicing mechanisms depending on tissue types. However, relative expression of the variants between tissues remained to be re-evaluated in mRNA level using RNA protection assay or quantitative RT-PCR, because the detected band intensities might include biased information derived from RT-PCR.

We constructed the full-length constructs for the four variants and expressed them in *Xenopus* oocytes (refer to "Materials and Methods") to compare their electrophysiological properties. Detectable inward currents were not recorded

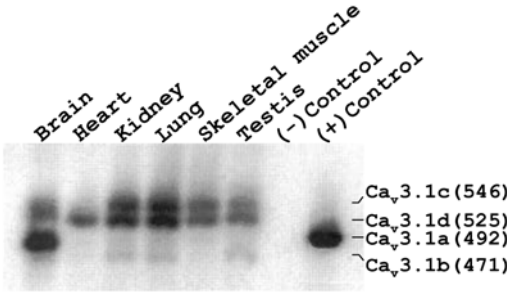

Fig. 2. Relative distribution of the four splice variant by Southern blot analyses. RT-PCR products amplified from total RNAs of rat brain, heart, kidney, lung, skeletal muscle, and testis were transferred on Nylon membrane and then probed with ^{32}P-labeled oligonucleotides specific to the rat $Ca_v3.1$ (refer to the method section). The negative control reaction did not include reverse transcriptase, and the positive control reaction included the reported rat $Ca_v3.1$ cDNA (Perez-Reyes et al., 1998) of which III-IV linker is identical to $Ca_v3.1a$.

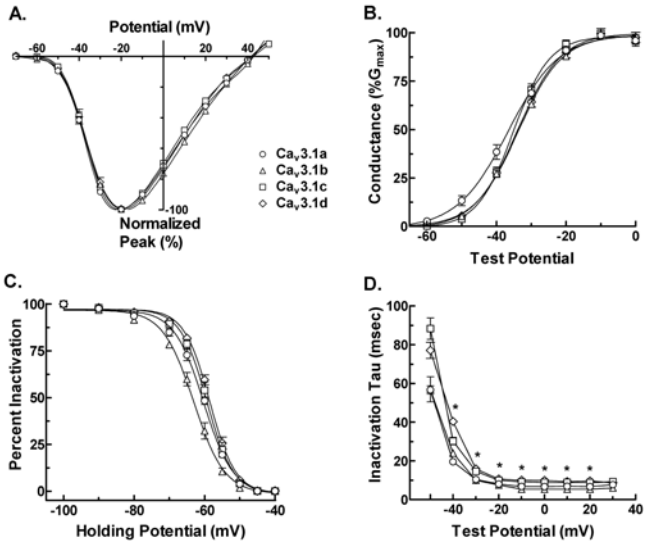

Fig. 3. Comparison of electrophysiological properties of the $Ca_v3.1$ variants. A. Normalized current-voltage (*I-V*) relationships of the four variants. Peak currents elicited by various test potentials from a holding potential of –90 mV were normalized to the maximum peak current pruduced at –20 mV, and their average percentages were plotted against test potentials. Symbols for $Ca_v3.1a$, $Ca_v3.1b$, $Ca_v3.1c$, and $Ca_v3.1d$ were open circles, triangles, squares, and diamonds, respectively. The data represent the means±SEM (n=7-17). B. Activation curves were obtained by plotting chord conductance (%*G*), calculated by dividing current amplitude by driving force (observed reversal potential minus the test potential) against test potentials. The curves are from fitting the data to the Boltzmann equation ($G=1/[1+\exp(V_{50}-V)/k]$), where V_{50} is the half-activation voltage (n=7-17). C. Each steady-state inactivation level was measured during voltage steps to –20 mV after 10 sec prepulses to potentials varying between 100 mV and -20 mV in 10 mV increments. The peak currents measured after 10 sec prepulses were normalized to the maximal current observed after a prepulse of –100 mV, and then the smooth curves are obtained from fitting the data to the Boltzmann equation (n=5-12). D. Currents evoked at various test potentials from a holding potential of -90 mV were fitted with two exponential curves and the time constants for inactivation were plotted against test potentials (n=7-17). The statistical differences were evaluated using one-way ANOVA.

from the control oocytes injected with H_20, whereas big inward currents were recorded from oocytes where cRNA of $Ca_v3.1a$, $Ca_v3.1b$, $Ca_v3.1c$, or $Ca_v3.1d$ was injected. To compare current-voltage-relationships and activation curves of the four variants, currents were elicited by a voltage protocol consisting of serial depolarizing voltage steps from –70 to +50 mV from a holding potential of 90 mV. The peak amplitudes were normalized to the maximum one which was detected at a test potential of –20 mV (Fig. 3A). It is likely that there are no significant differences between the current-voltage relationships of the four $Ca_v3.1$ variants. However, comparison of chord conductances of the four variants showed that the activation curve of $Ca_v3.1a$ was negatively shifted than $Ca_v3.1b$ or $Ca_v3.1d$ by about 3 mV (Fig. 3B). Evaluation of statistical significance using one-way ANOVA showed that the V_{50} value of $Ca_v3.1b$ or $Ca_v3.1d$ was significantly greater than that of $Ca_v3.1a$ (V_{50} values of $Ca_v3.1a$, $Ca_v3.1b$, $Ca_v3.1c$, and $Ca_v3.1d$ for activation=–36.67±0.60, –33.72±0.62, 35.17±0.43, 33.98±0.39 mV, respectively; $P<0.05$; n=7-17). Subsequent analyses of steady-state inactivation displayed that V_{50} of $Ca_v3.1b$ for steady-state inactivation was more smaller than those of the other splicing variants (V_{50} values for $Ca_v3.1a$, $Ca_v3.1b$, $Ca_v3.1c$, and $Ca_v3.1d$ for steady-state inactivation=–60.29±0.34, –63.08±0.33, 59.35 ±0.25, 58.54±0.25 mV, respectively; $P<0.05$, n=5-12, one-way ANOVA; Fig. 3C). Analyses of inactivation kinetics of the four variants displayed that the inactivation time constants of the four variants were significantly different one another at –40 mV, and the inactivation time constants of $Ca_v3.1a$ and $Ca_v3.1b$ were significantly smaller than those of $Ca_v3.1c$, or $Ca_v3.1d$ over test potentials bigger than –40 mV (n=7-17; Fig. 3D). These findings suggest that the splice variants differ in inactivation kinetics as well as the voltage dependence of steady-state inactivation.

Taken together, the distinctive expression pattern of the four variants shown by Southern blot analyses suggest that expression of the III-IV linker variants is tightly regulated depending on tissue types. Each splice variant with its unique electrophysiological properties may be involved in distinctive physiological roles in the tissues where each variant is expressed.

ACKNOWLEDGMENTS

This work was supported by Korea Research Foundation Grant funded by the Korean Government (KRF-2007-314-E00126), the Seoul R&BD Program (10816), and the Sogang University Research Grant (2008). Sang-Soo Lee and You-Mi Park are recipients of BK21 Predoctoral Fellowship and Ho-Won Kang is a recipient of BK21 Postdoctoral Fellowship.

REFERENCES

Bourinet E, Soong TW, Sutton K, Slaymaker S, Mathews E, Monteil A, Zamponi GW, Nargeot J, and Snutch TP (1999) Splicing of alpha 1A subunit gene generates phenotypic variants of P-and Q-type calcium channels. *Nat Neurosci* 2: 407-415.

Chen CC, Lamping KG, Nuno DW, Barresi R, Prouty SJ, Lavoie JL, Cribbs LL, England SK, Sigmund CD, Weiss RM, Williamson RA, Hill JA, and Campbell KP (2003) Abnormal coronary function in mice deficient in alpha1H T-type Ca^{2+} channels. *Science* 302: 1416-1418.

Chen L, Tian L, MacDonald SHF, McClafferty H, Hammond MSL, Huibant JM, Ruth P, Knaus HG, and Shipston MJ (2005) Functionally diverse complement of large conductance calcium-and voltage-activated potassium channel (BK) a-subunits generated from a single site of splicing. *J Biol Chem* 280: 33599-33609.

Chomczynski P and Sacchi N (1987) Single-step method of RNA isolation by acid guanidinium thiocyanate-phenol-chloroform extraction. *Anal Biochem* 162: 156-159.

Cribbs LL, Lee JH, Yang J, Satin J, Zhang Y, Daud A, Barclay J, Williamson MP, Fox M, Rees M, and Perez-Reyes E (1998) Cloning and characterization of á1H from human heart, a member of the T-type Ca^{2+} channel gene family. *Circ Res* 83: 103-109.

Gros L, Trapp S, Dabrowski M, Ashcroft FM, Bataille D, and Blache P (2002) Characterization of two novel forms of the rat sulphonylurea receptor SUR1A2 and SUR1BD31. *Br J Pharmacol* 137: 98-106.

Heron SE, Khosravani H, Varela D, Bladen C, Williams TC, Newman MR, Scheffer IE, Berkovic SF, Mulley JC, and Zamponi GW (2007) Extended spectrum of idiopathic generalized epilepsies associated with CACNA1H functional variants. *Ann Neurol* 62: 560-568.

Huguenard JR (1996) Low-threshold calcium currents in central nervous system neurons. *Annu Rev Physiol* 58: 329-348.

Jeong SW, Park BG, Park JY, Lee JW, and Lee JH (2003) Divalent metals differentially block cloned T-type calcium channels. *NeuroReport* 14: 1537-1540.

Kim D, Park D, Choi S, Lee S, Sun M, Kim C, and Shin HS (2003) Thalamic control of visceral nociception mediated by T-type Ca2+ channels. *Science* 302: 117-119.

Kim D, Song I, Keum S, Lee T, Jeong MJ, Kim SS, McEnery MW, and Shin HS (2001) Lack of the burst firing of thalamocortical relay neurons and resistance to absence seizures in mice lacking alpha(1G) T-type Ca(2+) channels. *Neuron* 31: 35-45.

Koshimizu T and Tsujimoto G (2006) Functional role of spliced cytoplasmic tails in P2X2-receptor-mediated cellular signaling. *J Pharmacol Sci* 101: 261-266.

Lee JH, Daud AN, Cribbs LL, Lacerda AE, Pereverzev A, Klockner U, Schneider T, and Perez-Reyes E (1999) Cloning and expression of a novel member of the low voltage-activated T-type calcium channel family. *J Neurosci* 19: 1912-1921.

Lee JH, Gomora JC, Cribbs LL, and Perez-Reyes E (1999) Nickel block of three cloned T-type calcium channels: Low concentrations selectively block α1H. *Biophys J* 77: 3034-3042.

Lory P, Bidaud I, and Chemin J (2006) T-type calcium channels in differentiation and proliferation. *Cell Calcium* 40: 135-146.

Nelson MT, Woo J, Kang HW, Vitko I, Barrett PQ, Perez-Reyes E, Lee JH, Shin HS, and Todorovic SM (2007) Reducing agents sensitize C-type nociceptors by relieving high-affinity zinc inhibition of T-type calcium channels. *J Neurosci* 27: 8250-8260.

Park JY, Ahn HJ, Gu JG, Lee KH, Kim JS, Kang HW, and Lee JH (2003) Molecular identification of Ca^{2+} channels in human sperm. *Exp Mol Med* 35: 285-292.

Perez-Reyes E (2003) Molecular physiology of low-voltage-activated t-type calcium channels. *Physiol Rev* 83: 117-161.

Perez-Reyes E, Cribbs LL, Daud A, Lacerda AE, Barclay J, Williamson MP, Fox M, Rees M, and Lee JH (1998) Molecular characterization of a neuronal low-voltage-activated T-type calcium channel. *Nature* 391: 896-900.

Suzuki S and Rogawski MA (1989) T-type calcium channels mediate the transition between tonic and phasic firing in thalamic neurons. *Proc Natl Acad Sci USA* 86: 7228-7232.

Takahashi SX, Mittman S, and Colecraft HM (2003) Distinctive modulatory effects of five human auxiliary β_2 subunit splice variants on L-type calcium channel gating. *Biophys J* 84: 3007-3021.

Vitko I, Chen Y, Arias JM, Shen Y, Wu XR, and Perez-Reyes E (2005) Functional characterization and neuronal modeling of the effects of childhood absence epilepsy variants of CACNA1H, a T-type calcium channel. *J Neurosci* 25: 4844-4855.

Welling A, Ludwig A, Zimmer S, Klugbauer N, Flockerzi V, and Hofmann F (1997) Alternatively spliced IS6 segments of the α1C gene determine the tissue-specific dihydropyridine sensitivity of cardiac and vascular smooth muscle L-type Ca^{2+} channels. *Circ Res* 81: 526-532.

[Received June 22, 2008; accepted September 1, 2008]